

This is the accepted manuscript made available via CHORUS. The article has been published as:

New resonances in $\pi\pi$

$\pi\pi$ above the $\pi\pi$ threshold investigated by inverse kinematic resonant scattering

Gurpreet Kaur, V. Guimarães, J. C. Zamora, M. Assunção, J. Alcantara-Nunez, A. L. de Lara, E. O. N. Zavallos, J. B. Ribeiro, R. Lichtenthäler, K. C. C. Pires, O. C. B. Santos, V. Morcelle, and R. J. deBoer

Phys. Rev. C **105**, 024609 — Published 17 February 2022

DOI: [10.1103/PhysRevC.105.024609](https://doi.org/10.1103/PhysRevC.105.024609)

New resonances in ^{11}C above the $^{10}\text{B}+p$ threshold investigated by inverse kinematic resonant scattering

Gurpreet Kaur¹, V. Guimarães¹, J. C. Zamora¹, M. Assunção², J.

Alcantara-Nunez¹, A. L. de Lara¹, E. O. N. Zevallos¹, J. B. Ribeiro¹, R.

Lichtenthäler¹, K. C. C. Pires¹, O. C. B. Santos¹, V. Morcelle³, and R. J. deBoer⁴

¹*Instituto de Física, Universidade de São Paulo, São Paulo 05508-090, Brazil.*

²*Departamento de Física, Universidade Federal de São Paulo,
Campus Diadema, São Paulo, Brazil.*

³*Departamento de Física, Universidade Federal Rural
do Rio de Janeiro, Rio de Janeiro, Brazil. and*

⁴*Department of Physics and the Joint Institute for Nuclear Astrophysics,
University of Notre Dame, Notre Dame, Indiana 46556, USA.*

(Dated: January 25, 2022)

Abstract

The spectroscopy of ^{11}C has been investigated by the resonant scattering of $^{10}\text{B}+p$ with the thick target inverse kinematic method. The $p(^{10}\text{B},p)^{10}\text{B}$ reaction was measured at $\theta_{\text{c.m.}} = 180^\circ$, 170° , 160° , 150° and 140° using a 35.93 MeV ^{10}B beam. Resonances in ^{11}C between the excitation energy of 9.6 and 11.8 MeV are observed. The excitation functions are compared with previous data using thin target, direct kinematics measurements. A multichannel R-matrix calculation, under the kinematics assumption of resonant elastic scattering, is performed and the resonant parameters such as the resonant energy E_x , the spin-parity J^π , and the proton-decay partial width Γ_p are extracted.

PACS numbers:

I. INTRODUCTION

Gaining insight into the structure of light radioactive nuclei, far from the valley of stability, has been the motivation of many experimental and theoretical studies in nuclear research [1, 2]. Such studies have established various new and unforeseen phenomena, such as halo structure [1], soft-excitation modes [3, 4], and rare β -delayed particle decays [5, 6], through the extensive studies of low lying states (below the particle threshold) with well-defined energies, spins and parities. However, still there are many open questions in near-threshold systems, in particular for light nuclei. For instance, the mirror nuclei ^{11}C and ^{11}B have a well-known level structure up to an excitation energy of 9.0 MeV, but there are discrepancies and uncertainties about the existence of resonances and their spin-parity assignment above the proton threshold. Recently, a resonance at 11.42 MeV (200 keV above the $^{10}\text{Be}+p$ threshold) in ^{11}B has been associated with a possible β -delayed proton emission decay of ^{11}Be with implications for dark matter production [7, 8]. The mirror nuclei have a correspondence between the level spins and parities due to their similar nucleon number and the charge independence of the nuclear force, and therefore the existence of a level in ^{11}B must have a corresponding partner in ^{11}C . There are experiments suggesting the possibility of ^{11}C having a resonance around the region of 11.0 MeV excitation energy, but this hypothesis has not been confirmed yet.

The resonance structure in ^{11}C has important implications for the following three reactions:

- (1) $^7\text{Be}(\alpha, \gamma)$ for astrophysics in the hot pp -chain of Sun [9, 10],
- (2) $^{10}\text{B}(p, \alpha)^7\text{Be}$ as the contamination of the candidate of aneutronic fusion reaction $^{11}\text{B}(p, 2\alpha)^4\text{He}$ [11] and
- (3) $^{10}\text{B}(p, \gamma)$ as a competing reaction for the $^{10}\text{B}(p, \alpha)^7\text{Be}$ channel.

Therefore, experimental data of resonance states in ^{11}C above the $^{10}\text{B}+p$ threshold offers an excellent method to study the properties of the above reaction channels. Previous experiments, performed in forward kinematics, using a proton beam on enriched ^{10}B targets, are reported in Ref. [12] where the most backward angle measured is at $\theta_{\text{c.m.}} = 170^\circ$. A systematic analysis of these data using the R-matrix formalism [13, 14] was recently performed by Wiescher *et al.* [11], which shows two dominated resonances at the $E_x = 10.08$ ($7/2^+$) and 10.68 ($9/2^+$) MeV in ^{11}C . However, the level density of ^{11}C , above the proton

threshold ($E_x=8.6894$ MeV), starts to increase rapidly and the levels are described by large particle widths, on the order of hundreds of keVs. This has made the determination of the level scheme for this nucleus quite challenging and the level properties above $E_x = 11.0$ MeV are particularly uncertain. Additional data, obtained with a different experimental technique such as inverse kinematics would help to improve the spectroscopic information on this nucleus. The resonances may be more pronounced at $\theta_{\text{c.m.}} = 180^\circ$, in the inverse kinematic frame of reference, which are not feasible in a forward kinematics approach. The Thick Target in Inverse Kinematics (TTIK) technique [15, 16] allows to extract the excitation function spectra in a wide energy range at backward angles (including $\theta_{\text{c.m.}} = 180^\circ$) in a single measurement. In this work, we used the TTIK method for the measurement of ^{10}B on protons excitation function to investigate the resonances in ^{11}C above the $^{10}\text{B}+p$ threshold.

The article is organized as follows. The experimental details are described in Sec. II, the data analysis method and results are discussed in Sec. III and finally, summary and conclusion are presented in the last section.

II. EXPERIMENTAL DETAILS

The reaction channels of the $^{10}\text{B}+p$ system have been studied with the low-energy Radioactive Ion Beams in Brazil (RIBRAS) facility [17, 18], installed at the 8-UD Pelletron Tandem of the University of São Paulo. The measurements were performed using the TTIK method [15, 16] to obtain excitation functions for ^{11}C at backward angles in the center of mass system. In this method, the target is thick enough to stop the beam particles but allows the light, p and α , particles to be detected. In the present case, the beam lost energy from $E_{\text{c.m.}} = 0$ MeV to 3.3 MeV while penetrating the target. A pure ^{10}B beam was obtained from the Pelletron accelerator at an energy of $E_{\text{lab}} = 38.4$ MeV. To avoid the deterioration of the plastic foil due to relatively high intensity of the primary beam, an ^{27}Al foil (4.6 mg/cm^2) was mounted at the production target of the RIBRAS system to scatter the incident beam. The scattered ^{10}B particles were then refocused by a superconducting solenoid of the RIBRAS system into the plastic target in the scattering chamber (after the solenoid). In this way, only scattered particles from 3° to 6° were accepted. Thus the beam-production target acts as an intensity degrader, producing an elastically scattered ^{10}B beam at $E_{\text{lab}} = 37.2$ MeV with an intensity of 10^7 pps. Another important advantage of

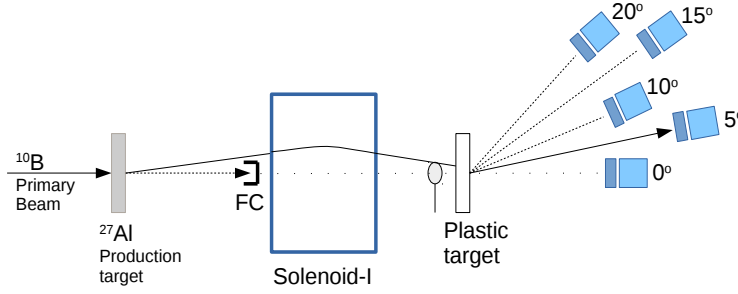


FIG. 1: (Color online) A schematic view of the experimental setup.

the present technique is to have a beam intensity readout by using a Faraday Cup (FC) right at the entrance of the solenoid to collect the most forward scattered particles (0° to 3°) and the unreacted beam. A schematic view of the experimental setup is shown in Fig. 1. The target holder in the scattering chamber consisted of three targets: a ^{197}Au foil 1.25 mg/cm² thick, a natural carbon foil 15 mg/cm² thick and a polyethylene plastic foil $[\text{CH}_2]_n$ 100 μm thick. A thin ^{197}Au foil (1.58 mg/cm²) was placed in front of the plastic target to measured ^{10}B back scattering events. However, due to experimental set-up constraints, they could not be measured. The beam energy hitting the entrance surface of the plastic target (after the thin ^{197}Au foil) was 35.93 MeV. The measurement with ^{197}Au target was used for calibration purposes. Elastic scattering on this target at 20° was measured between runs during the whole experiment. This data, along with the integrated charge of the primary beam (collected at Faraday Cup), was utilized to normalize the intensity of the scattered beam and it was quite constant during the measurement (about 10^7 pps). Measurements with the natural carbon target were also performed to subtract the contribution from the reactions of the ^{10}B beam with the carbon present in the polyethylene foil.

The scattered particles from the reaction target were detected with ΔE -E silicon telescopes placed at laboratory angles of $\theta_{\text{lab}} = 0^\circ, 5^\circ, 10^\circ, 15^\circ$ and 20° with respect to the beam axis. These telescopes, comprised of silicon surface barrier detectors of 50 μm and 1000 μm thickness, respectively, covered a geometric solid angle of 8.70 msr. The detectors in the telescopes were calibrated using α -source measurements. The energy resolution of the ^{10}B beam (from ^{197}Au run) was approximately 410 keV, which corresponds to a proton energy resolution of 41 keV. The great advantage of the method is the good energy resolution, which does not depend strongly on the energy resolution of the incident beam. We have used the Lise++ code [19] for the energy loss correction of the proton. The higher edge of

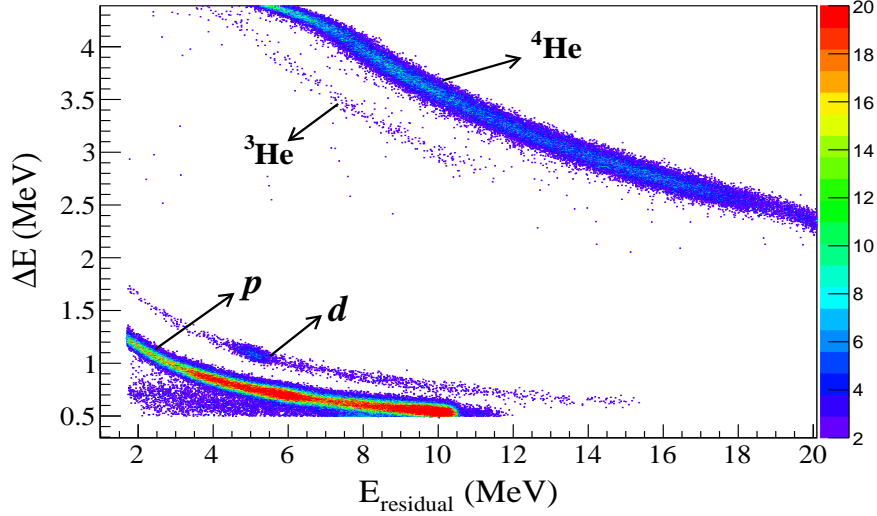


FIG. 2: (Color online) Two-dimensional spectrum (ΔE vs E_{residual}) measured at $\theta_{\text{lab}} = 0^\circ$. The measured light particles p , d , ^3He and ^4He are indicated.

$E_{\text{c.m.}}$, from the spectra was in good agreement with expected measured $E_{\text{c.m.}}$ energy of the beam energy at the front surface of the target. The entrance angle of the primary beam in the solenoid was between 3° to 6° causing an angular divergence of the refocused ^{10}B beam. This effect was investigated using a simulation of the RIBRAS system [20] using the Geant4 toolkit [21]. The angular divergence of the refocused ^{10}B beam is about 1° (FWHM) at the target position, and it produces a straggling in the energy of about 100 keV which is already embedded in the final energy resolution.

III. ANALYSIS AND RESULTS

A. Deduction of excitation functions

The advantage of the present measurement, in comparison with backscattering at forward kinematic, is the online beam intensity readout. The proportionality of the readout of ^{10}B beam from the Faraday Cup and the scattered ^{10}B beam, refocused on the polyethylene target, was kept practically constant during the experiment. This allow us to precisely measured the intensity of the incident beam, hence reducing the error in the extracted excitation function. The two dimensional particle identification spectrum ΔE - E , obtained

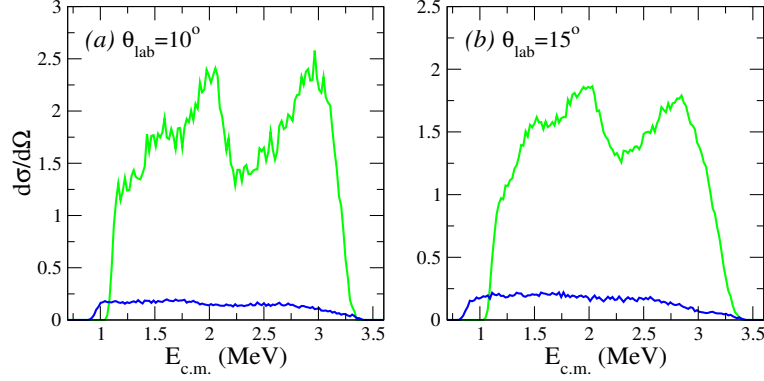


FIG. 3: (Color online) Proton spectra excitation function obtained with the plastic target (green) and ^{12}C target (blue) (background events) at $\theta_{\text{lab}} = 10^\circ$ (a) and 15° (b).

at $\theta_{\text{lab}} = 0^\circ$, is shown in Fig. 2. As illustrated, ^4He ($Q = +1.1457$), ^3He ($Q = -0.5332$) particles and p ($Q = 0$ MeV) coming from $^{10}\text{B}+p$ reaction are well separated. The bands for deuterons and tritons are also observed, which may be coming from reaction of ^{10}B with ^{12}C target as the Q -value for $^{10}\text{B}(p,d)$ and $^{10}\text{B}(p,t)$ are -6.2125 MeV and -18.5317 MeV, respectively.

The background contribution of protons from the reaction of ^{10}B with carbon nucleus, also present in the plastic target, is perfectly removed through separate measurements with a pure ^{12}C target, using the same ^{10}B beam and under the same experimental conditions. The background contribution is found to be an order of magnitude smaller compared to the protons of interest and the background spectra has a slowly varying energy dependence, as shown in Fig. 3. The thickness of the ^{12}C target was taken in such a way that the observed proton spectra span about the same energy range as that obtained with the plastic target. The background was not measured at 0° and 5° since the ^{10}B beam was not completely stopped inside the carbon foil at these angles. The background at these two angles was obtained by extrapolation of the measurements at other angles. The integral of background counts at 10° , 15° and 20° were fitted with a linear function and extrapolated for 0° and 5° . Then the ratio of the integral value for 0° (and 5°) and that of 10° was multiplied with the measured background spectra at 10° to estimate the background spectra for 0° (and 5°).

The proton spectra obtained from the $p(^{10}\text{B},p)^{10}\text{B}$ resonant scattering, with energy loss correction and background subtraction, are shown in Fig. 4. The energy range of the proton spectra investigated in the present work is $E_{\text{c.m.}} = 1.2$ to 3.3 MeV, which corresponds to

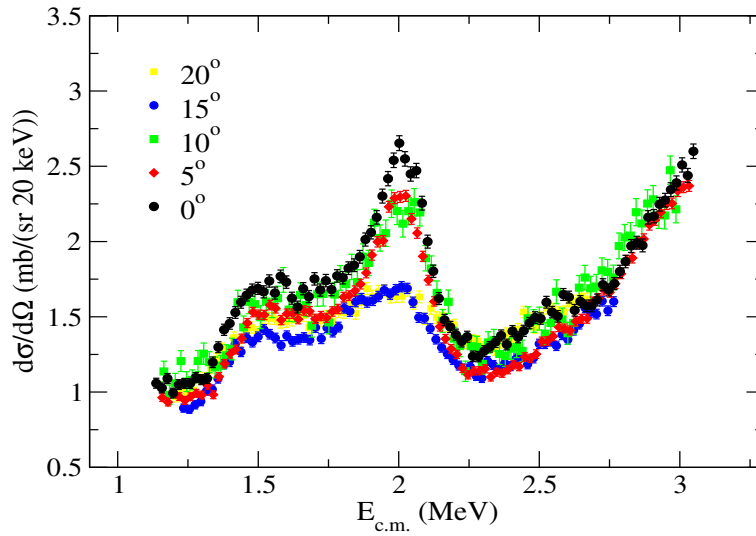


FIG. 4: (Color online) The extracted excitation function for the reaction channel $^{10}\text{B}(p,p)^{10}\text{B}$ at indicated lab angles.

excitation energy of 9.7 to 11.9 MeV in ^{11}C . The level scheme of ^{11}C in this excitation energy range is shown in Fig. 5. One should note that above the proton threshold ($S_p = 8.6987$ MeV) the spin assignment for the levels is not well established. Also, as can be seen in the Fig. 5, the level scheme of ^{11}C is quite complex.

B. Comparison with previous results

Proton spectra data from direct kinematics (backscattering) of proton beam on ^{10}B target is reported in Chiari et al. [12]. The comparison of the excitation function of the present inverse kinematics with the direct kinematics data is shown in Fig. 6, where a good agreement, for the most forward angles, is observed up to 2.5 MeV. The resonances in the inverse kinematic are broader compared to those observed in the direct kinematic data, and they get broader at the spectra measured in angles far from $\theta_{\text{lab}} = 5^\circ$ ($\theta_{\text{lab}} = 170^\circ$ direct kinematic). In the laboratory frame and in inverse kinematics, the center of mass angular range gets compressed from 180° into just the forward 90° . The consequence of this is that the cross-section will be very sensitive to angle of the measurement, and any uncertainty in the detector angle could cause some difference in the spectra. Also, the solid angle of the detector covers a much broader angular range in the center of mass frame compared to the lab frame. The former seems to be not so significant in the present work because the low energy resonance

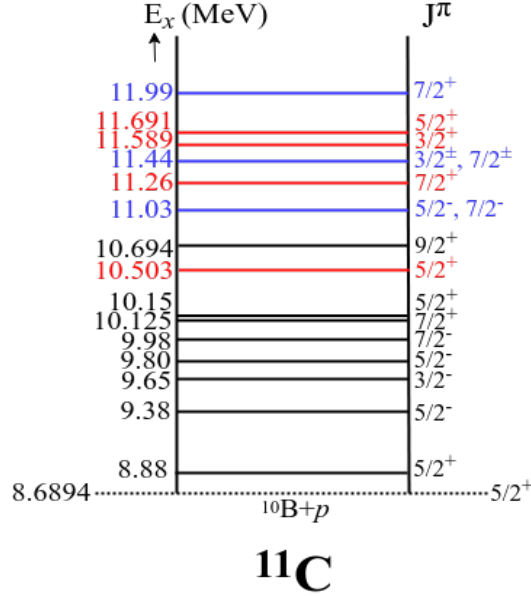


FIG. 5: (Color online) Energy level diagram of the ^{11}C nucleus above the proton separation energy (indicated with the dotted line). The values in black color correspond to the levels reported in the Ref. [11], in blue are resonances reported in the references tabulated in Table I and in red the new resonances observed in the present work.

peaks in the present case are coinciding with those observed in Chiari et al. [12], but the latter can be a possible contribution for the broadening of the resonances.

Also, as can be observed in Fig. 6, there is some discrepancy in the higher energy region (above 2.5 MeV). To better understand this discrepancy, we first checked the influence of energy loss, since, in the present method, the derived cross section is very sensitive to the stopping power. Also, the energy loss correction is an important issue to properly obtain the proton spectra. We calculated the stopping power and energy loss with the Lise++ platform [19]. By changing the value of energy loss by $\pm 40\%$ a little influence on the proton spectra was observed. We also ruled out possible beam contaminants since the refocused scattered ^{10}B is obtained as a clean beam in the elastic scattering spectra measured with ^{197}Au target. Additionally, we also estimated the possible inelastic scattering contribution. The inelastic scattering would occur for $E_p > 790$ keV in direct kinematic. However, as observed in Ref. [24], the inelastic scattering cross-section, due to the excitation of the ^{10}B projectile or ^{12}C target, in the energy range of the present measurement is low (3 to 6 order of magnitudes

TABLE I: Resonance properties for ^{11}C above $E_x = 11$ MeV, available in literature.

E_x (MeV)	J^π	Γ_p (keV)	Ref.
11.03	$5/2^-, 7/2^-$	–	[9]
11.26	$7/2^+$	192	[22]
11.44	$3/2^\pm, 7/2^\pm$	–	[9]
11.99	$7/2^+$	467(112)	[23]

lower as compared to measured cross-section) and flat. We, thus, can consider that inelastic scattering would not have any structure and would not make any influence in the energy spectra of the present work. Although the discrepancy in the normalization between direct and inverse kinematic data for the energy region above $E_{\text{c.m.}} = 2.5$ MeV is not trivial, there is a clear indication of a resonance for the proton at energy between $E_{\text{c.m.}} = 3.0$ and 3.5 MeV in our spectra. This resonance is observed in the excitation function for the proton capture reaction reported in Fig. 6 of Ref. [25], with a higher cross section higher than the resonance at $E_{\text{c.m.}} = 2.0$ MeV.

Although we could not achieve the same energy resolution as the forward kinematics measurement for angles other than 180° degree, our approach allowed a better normalization determination. The measurement at 5° in inverse kinematic (compared to the 170° at forward kinematic) has similar resolution. The resolution is better, and about the same as direct measurements, for the 0° excitation function. Moreover, the present data was shifted by 30 keV towards the low energy side to match the peak positions of Chiari’s data. This shift may be due to uncertainty in the energy calibration. On the other hand, the excitation functions of Chiari et al. [12] has some systematic uncertainty and were normalized to present data using a factor of 0.92 (obtained from the prominent peaks).

C. R-matrix calculations

To further investigate the resonances in ^{11}C , the measured excitation function in the range of 1.2 to 3.3 MeV ($E_x = 9.9$ to 11.7 MeV) has been analyzed with the multichannel R-matrix code AZURE2 [13]. The level structure of the ^{11}C nucleus in this energy range (above the proton threshold) is quite complex, as shown in Fig. 5. The complexity of level structure of

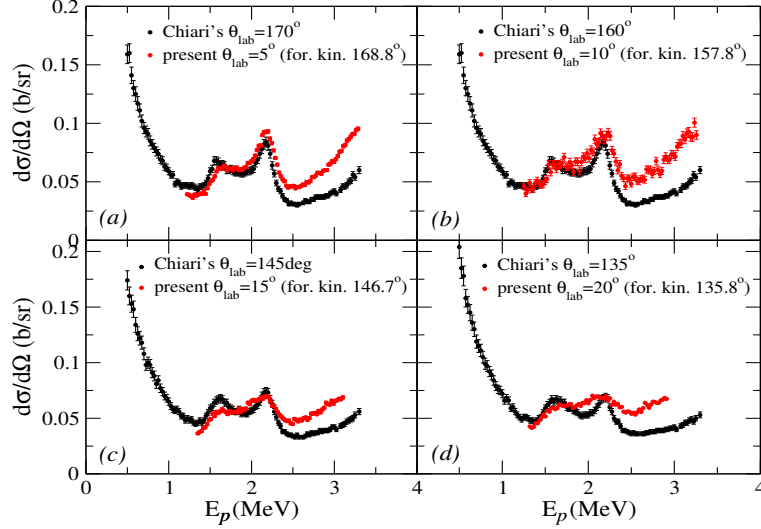


FIG. 6: (Color online) Excitation functions measured in the present work compared with the one obtained in direct kinematic reported by Chiari *et al.* [12]. The corresponding angles are mentioned in the lab frame and the equivalent lab angles from inverse to forward kinematics are given inside the square brackets.

^{11}C nucleus has already been observed in the $^{10}\text{B}(p,\gamma)^{11}\text{C}$ proton capture reaction [26], where strong, broad and interfering resonances were observed. The previous direct kinematic data for $^{10}\text{B}(p,p)$ by Chiari *et al.* [12], measured in the energy range of 0.5 to 2.3 MeV, have also observed strong resonances. The proton spectra obtained from Chiari's experiment were recently analyzed with R-Matrix by M. Wiescher *et al.* [11]. In their analysis, although two strong and prominent peaks at $E_x = 10.08$ ($7/2^+$) and 10.68 MeV ($9/2^+$) dominate the spectra, some other broad resonance at $E_x = 10.10$ MeV ($5/2^+$) and $E_x = 9.98$ MeV ($7/2^-$) were included in the fitting, giving overall good results. The low energy region of the spectra (below 1.0 MeV) is dominated by the Coulomb scattering. It is important to mention that in the analysis of direct kinematics data up to $E_{\text{c.m.}} = 2.2$ MeV in Ref. [11], the contribution of inelastic scattering (due to the excitation of the first excited state of ^{10}B at 718 keV) was considered negligible. This assumption is based on the results of the analysis reported in Ref. [27]. However, another work by Bernstein *et al.* [24] has shown that the inelastic cross-section flattens out above 2.5 MeV and is almost constant up to 3.5 MeV. We have calculated the cross-section for elastic and elastic+inelastic channel, separately, in the AZURE2 code (without fitting the data set), and the observed cross-sections for the

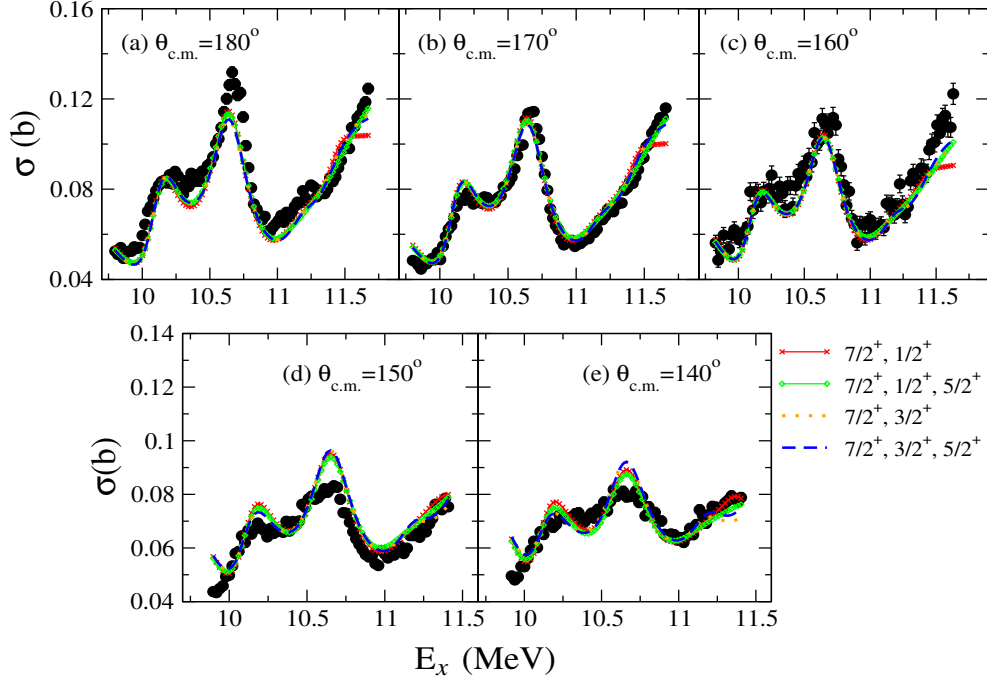


FIG. 7: (Color online) R-matrix fits to the present data with a simultaneous calculations for including all the measured angles. The resonant energy levels considered above 11.0 MeV are: 11.26 MeV, 11.44 MeV, and 11.75 MeV. The corresponding spin-parity combinations for these three levels are shown with legends.

two cases are nearly identical up to $E_{c.m.} = 3.5$ MeV. Thus, in the present analysis we have neglected the contribution from the inelastic scattering.

The simultaneous fitting of the spectra measured at all angles are shown in Fig. 7. The starting values of energies and spin-parity in the fitting procedure were considered from the previous R-matrix calculations of direct kinematics data [11]: $E_x = 9.98$ ($7/2^-$), 10.125 ($7/2^+$), 10.15 ($5/2^+$), 10.694 MeV ($9/2^+$). Since the range of our spectra extends to somewhat higher energy than the previous data, a few extra resonances above 11.0 MeV were included: $E_x = 11.03$, 11.26, 11.44 and 11.75 MeV. The resonance at 11.26 MeV was previously proposed in the literature [22]. This resonance was actually reported in the old compilation for $A=11$ nuclei in Ref. [28]. In the new compilation for ^{11}C [9], the resonances at $E_x = 11.03$ MeV and 11.44 MeV, with spin-parity $J^\pi = 5/2^-$ or $7/2^-$ and $3/2^\pm$ or $7/2^\pm$, respectively, are proposed. The energies of these resonances were kept fixed during the fitting process. The resonance at 11.75 MeV has been included based on the spectrum measured at $\theta_{c.m.} = 180^\circ$.

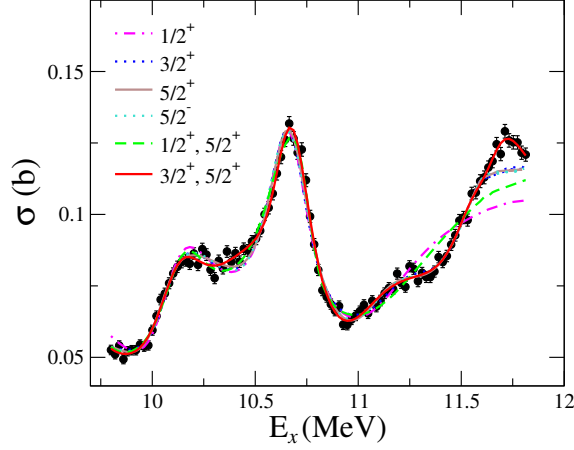


FIG. 8: (Color online) The R-matrix calculation for $^{10}\text{B}(p,p)$ reaction for the data measured at $\theta_{\text{c.m.}} = 180^\circ$ in the inverse kinematics. The results with different spin-parity combination for a resonances at $E_x = 11.44$ MeV and 11.75 MeV (considered as variable parameters) are shown.

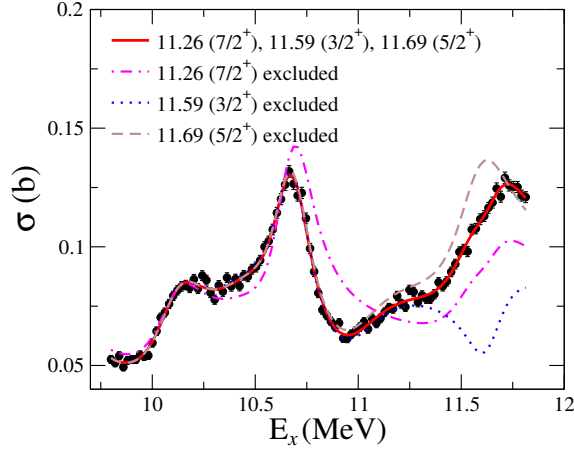


FIG. 9: (Color online) Role of three proposed resonances in the best fit: the results shown are obtained by excluding one at a time as indicated with the legends.

All the previous proposed resonances for ^{11}C above $E_x = 11.0$ MeV in the literature are listed in Table I. We have tried considering all these states in the R-matrix fitting procedure. For all the spectra measured at different angles, the number of dependent variables are large and it is very difficult to get a conclusive result. To minimize the number of fit parameters we fixed the energies of the all resonances to values mentioned above, however, the partial widths were allowed to vary. The experimental resolution of 41 keV (in c.m. frame) and channel radius of 4.4 fm were considered in the AZURE2 code. The results of such calculations

can be seen in Fig. 7. After trying different possible assignments for the two resonances at $E_x = 11.26$ and 11.44 MeV, the best fit gave $7/2^+$ and $1/2^+$ or $3/2^+$, respectively, as indicated in Fig. 7. The addition of the resonance at $E_x = 11.03$ MeV does not show any significant effect on the resonance structure, hence it was ignored. The states with E_x below 9.0 MeV were tested and showed negligible influence onto the present energy range spectra. They were not considered in the final results shown in Fig. 7. A resonance at 11.75 MeV (fixed value) was considered to better reproduce the high energy part of the spectra. For a consistent analysis, the spectra measured at $\theta_{\text{c.m.}} = 160^\circ$, 170° and 180° were truncated at the proton center of mass energy of 3.1 MeV. The spectra measured at 140° and 150° were truncated at lower proton energy (2.5 MeV) due to the larger energy loss as the target gets thicker. This truncation produced different ranges in the spectra shown in Fig. 7 as a function of excitation energy of ^{11}C . Since the spectrum at $\theta_{\text{c.m.}} = 180^\circ$ was measured up to the energy of 11.8 MeV, an indication of a resonance at $E_x = 11.75$ MeV can be observed. After trying different assignments, the spin-parity $5/2^+$ for this resonance gave a reasonable fit for all spectra. From our analysis, any negative parity for the three new resonances above 11.0 MeV (11.26 , 11.44 and 11.75 MeV) are completely ruled out.

By taking a closer look at the spectra shown in Fig. 7, one can see that the results for the strong resonance at 10.68 MeV are different in the spectra measured at different angles. The overall calculation underestimated the 180° data, reasonably fitted the 170° and 160° data, and overestimated the remaining angles, 150° and 140° . This might give an indication that the height of the resonance peaks, which are in turn related to the broadening of the peaks, is dependent upon the detector angle in center of mass. In fact, the present data is measured in inverse kinematics and the AZURE2 code only treats data in the direct kinematics. We have, thus, converted the inverse kinematics data to the center of mass system, and then convert to direct kinematics energies, considering the energy axis in terms of excitation energy of ^{11}C . We have to consider that there is a broadening of the peaks due to the angular opening of the detector. This broadening effect should be much less pronounced for zero degree ($\theta_{\text{c.m.}} = 180^\circ$ in the center of mass frame) measurement as compared to the other angles measurements, since it covers the plus and minus direction.

Since we expected a better resolution for the measurement performed at ($\theta_{\text{c.m.}} = 180^\circ$), we performed an independent analysis for the spectrum measured at this angle. For this analysis, we extended the energy range of this spectrum as compared to the one in the

simultaneous analysis shown in Fig. 7. In this case, we are dealing with a single data set and the dependent parameters are reduced. We, hence, considered the energy values and partial widths (for resonances above 11.0 MeV) as variable parameters and different spin-parity combinations are tried for the full range spectrum. A test for $E_x = 11.26$ MeV resonance indicated the negative parity assignment should be ruled out and $J^\pi = 7/2^+$ gave the best result. The calculation also shows that $1/2^+$ spin parity for the resonance around 11.44 MeV (initial value) is not able to explain the higher energy part. However good fits are obtained with $5/2^\pm$ or $3/2^\pm$. In fact, the resonance structures obtained with $5/2^+$ (or $3/2^+$) and $5/2^-$ (or $3/2^-$) are similar with almost the same value of best fitted E_x . The best fit to the spectra having minimum chi-square, shown with the solid red line in Fig. 8, is obtained by adding the state at $E_x = 11.75$ MeV (considered as variable) with spin parity as $5/2^+$ and with $3/2^+$ spin parity for 11.44 MeV state.

The parameter values obtained from the best fit are quoted in Table II. The resonance with initial energy of 11.44 MeV changed to 11.589 MeV and the resonance at 11.75 changed to 11.691 MeV. The importance of the presence of these resonances were tested and the result is shown in Fig. 9. The lower resonances reported in Wiescher's paper [11] showed a significant influence on the spectrum considered here, their role is checked considering one at a time. While performing the calculations, we observed that an improved results is obtained if we replace the the resonance at 10.15 MeV ($5/2^+$), mentioned in Wiescher's paper [11], by 10.503 MeV ($5/2^+$). The excitation energy of the isobaric analog states in ^{11}B can be calculated from the resonance energy, $E_{\text{c.m.}}$, as

$$E_x = E_{\text{c.m.}} + S_n - \Delta E_C, \quad (1)$$

where $S_n = 11.45$ MeV is the neutron separation energy and ΔE_C is the Coulomb displacement energy that is assumed to be 2.2 MeV. This is consistent with the reduction in the Coulomb energy difference observed in ^{11}C and ^{11}B due to the strong cluster configuration of the high energy states [23]. Fig. 10 shows a diagram of the mirror states obtained in this study. The proposed states are consistent with the values reported in other works [29], in particular with the $^7\text{Li}(\alpha, p)$ and $^7\text{Be}(\alpha, p)$ experiments of Yamaguchi et al. [9, 30]. They reported a $5/2^+$ state in ^{11}B at 11.063 MeV that is consistent with the analog state in ^{11}C at 10.503 MeV ($5/2^+$) proposed in the present work.

We have tested the consistency of the results by performing R-matrix calculation con-

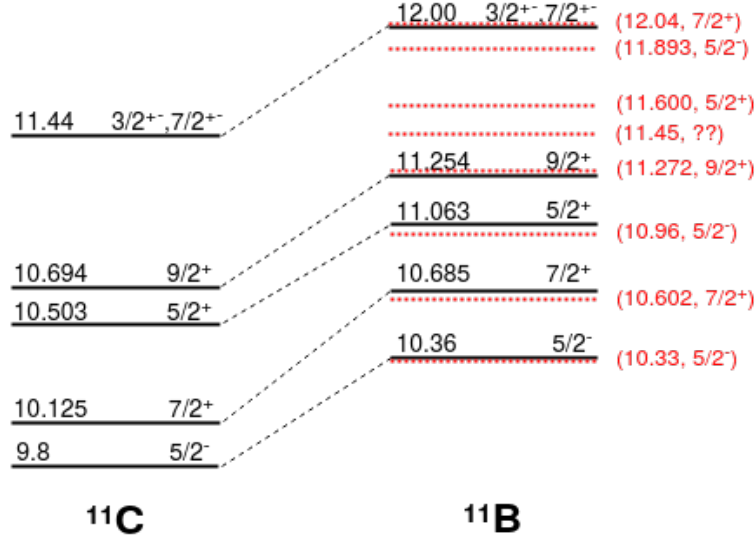


FIG. 10: The observed resonant states in ^{11}C and together with those obtained with eq. (1) for the mirror analog to ^{11}B states. For each state, E_x in MeV and J^π are mentioned. The states reported in literature [29] for the ^{11}B are shown with red dotted lines and corresponding resonant parameters are mentioned in red.

sidering the final results obtained for the $\theta_{\text{c.m.}} = 180^\circ$ spectrum to the other spectra. The results by fixing the spins and leaving the energy and width to vary, indicate that the spin assignment is consistent but there is a small variation in the energy within 100 keV.

IV. SUMMARY AND CONCLUSION

The energy region between $E_{\text{c.m.}} = 1.2$ MeV and 3.3 MeV, corresponding to the excitation energy of $E_x = 9.6$ and 11.8 MeV in ^{11}C , above the $^{10}\text{B}+p$ threshold, has been scrutinized with single incident energy using the method of thick target in inverse kinematics. From the R-matrix analysis considering all spectra measured, the previous resonances at $E_x = 9.98$ ($7/2^{-}$), 10.125 ($7/2^{+}$), 10.15 ($5/2^{+}$), 10.694 MeV ($9/2^{+}$), were considered plus the three new resonances above the 11.0 MeV: $E_x = 11.26$ ($7/2^{+}$), 11.44 ($3/2^{\pm}$ or $7/2^{\pm}$) and 11.75 ($5/2^{+}$) MeV. Considering the R-matrix analysis only for the spectrum measured at $\theta_{\text{c.m.}} = 180^\circ$ the values for the three new proposed resonances are slightly different, namely, $E_x = 11.26$ ($7/2^{+}$), 11.589 ($3/2^{+}$) and 11.691 ($5/2^{+}$) MeV. From our result, a lower resonance previously reported at $E_x = 10.15$ MeV ($5/2^{+}$) seemed to have an excitation energy of $E_x =$

TABLE II: Proposed resonance properties for ^{11}C obtained from the best fit.

E_x (MeV)	J^π	(s, l)	Γ_p (keV)
10.503	$5/2^+$	(5/2, 0)	275.1
		(5/2, 2)	350.5
		(7/2, 2)	7.6
11.26	$7/2^+$	(5/2, 2)	347.9
		(7/2, 0)	20.5
		(7/2, 2)	711.9
11.589	$3/2^+$	(5/2, 2)	0.6
		(7/2, 2)	301.1
11.691	$5/2^+$	(5/2, 0)	64.1
		(5/2, 2)	105.7
		(7/2, 2)	180.2

10.503 MeV. This proposed value of E_x nicely follows the trend for the structure of mirror nucleus ^{11}B .

The presence of a resonance at 11.42 MeV in ^{11}B has been used to explain the branching ratio observed in the β -delayed proton emission of ^{11}Be [31]. From our results, the corresponding mirror analog of this resonance in ^{11}C , considering the Coulomb displacement, would be at about 11.00 MeV. However, as already mentioned, the addition of the resonance at $E_x = 11.03$ MeV in the R-matrix calculation does not show any significant improvement in the fit, hence it was ignored.

Moreover, the present work reveals that while doing such inverse kinematic measurements, the angular coverage should be as small as possible to reduce the broadening of peaks in the resonance structure. In fact, the present study requires the inclusion of the solid angle of the detector in the experimental effects in AZURE2 program to extract the precise results from the data. This is particularly important while doing the R-matrix calculations for the data measured in inverse kinematics.

From the present work, we conclude the validation of the data measured with TTIK

technique with respect to the direct kinematics data. This method will be further useful to investigate the complex resonance structure of other exotic nuclei such as ^{11}B through a $^{10}\text{Be}+p$ resonant elastic scattering measurement, which is our planned future work.

V. ACKNOWLEDGMENT

This work was financially supported by São Paulo Research Foundation (FAPESP)(Grant No. 2016/17612-7, 2018/18241-8, 2018/04965-4, 2019/07767-1 and 2019/02759-0) and by the Conselho Nacional de Desenvolvimento Científico e Tecnológico (CNPq) Proc. No. 304961/2017-5 and INCT-FNA Proc. No. 464898/2014-5. RJD acknowledges support from the National Science Foundation through Grant No. Phys-2011890, and the Joint Institute for Nuclear Astrophysics through Grant No. PHY-1430152 (JINA Center for the Evolution of the Elements).

-
- [1] I. Tanihata, H. Savajols, and R. Kanungo, *Prog. Part. Nucl. Phys.* **68**, 215-313 (2013).
 - [2] J.J. Kolata, V. Guimaraes, and E.F. Aguilera, *Eur. Phys. J. A* **52**, 123 (2016).
 - [3] S. A. Fayans, *Phys. Lett. B* **267**, 443-446 (1991).
 - [4] H. Sagawa, *Nucl. Phys. A* **538**, 619c (1992).
 - [5] B. Blank and M.J.G. Borge, *Prog. Part. Nucl. Phys.* **4560**, 403 (2008).
 - [6] M. Pfützner, M. Karny, L.V. Grigorenko, and K. Riisager, *Rev. Mod. Phys.* **84**, 567 (2012).
 - [7] Y. Ayyad, B. Olaizola, W. Mittig, G. Potel, V. Zelevinsky, M. Horoi, S. Beceiro Novo, M. Alcorta, C. Andreoiu, T. Ahn, M. Anholm, L. Atar, A. Babu, D. Bazin, N. Bernier, S.S. Bhat-tacharjee, M. Bowry, R. Caballero-Folch, M. Cortesi, C. Dalitz, E. Dunling, A.B. Garnsworthy, M. Holl, B. Kootte, K.G. Leach, J.S. Randhawa, Y. Saito, C. Santamaria, P. Siuryte, C.E. Svensson, R. Umashankar, N. Watwood, and D. Yates, *Phys. Rev. Lett.* **123**, 082501 (2019).
 - [8] A. Volya, *Europhysics Lett.* **130**, 12001 (2020).
 - [9] H. Yamaguchi, D. Kahl, Y. Wakabayashi, S. Kubono, T. Hashimoto, S. Hayakawa, T. Kawabata, N. Iwasa, T. Teranishi, Y.K. Kwon, D.N. Binh, L.H. Khiem, and N.N. Duy, *Phys. Rev. C* **87**, 034303 (2013).
 - [10] M. Wiescher, J. Görres, S. Graff, L. Buchmann, and F.K. Thielemann, *Astrophys. J.* **343**, 352

- (1989).
- [11] M. Wiescher, R.J. deBoer, J. Görres, and R.E. Azuma, *Phys. Rev. C* 95, 044617 (2017).
 - [12] M. Chiari, L. Giuntini, P. Mando, and N. Taccetti, *Nucl. Instrum. Methods Phys. Res. B* 184, 309 (2001).
 - [13] R.E. Azuma, E. Uberseder, E.C. Simpson, C.R. Brune, H. Costantini, R.J. deBoer, J. Görres, M. Heil, P.J. LeBlanc, C. Ugalde, and M. Wiescher. *Phys. Rev. C* 81, 045805 (2010).
 - [14] A.M. Lane and R.G. Thomas, *Rev. Mod. Phys.* 30, 257 (1958).
 - [15] K.P. Artemov, O.P. Belyanin, A.L. Vetoshkin, R. Wolski, M.S. Golovkov, V.Z. Goldberg, M. Madeja, V.V. Pankratov, I.N. Serikov, V.A. Timofeev, V.N. Shadrin, and J.Szmider, *Sov. J. Nucl. Phys.* 52, 408 (1990).
 - [16] M. Benjelloun, Th. Delbar, W. Galster, P. Leleux, E. Liénard, P. Lipnik, P. Duhamel, J. Vanhorenbeeck, C. Rolfs, G. Roters, H.P. Trautvetter, and W. Rodney, *Nucl. Instrum. Meth. Phys. Res. A* 321, 521-528 (1992).
 - [17] R. Lichtenthäler, A. Lépine-Szily, V. Guimarães, C. Perego, V. Placco, O. Camargo Jr., R. Denke, P.N.de Faria, E.A. Benjamim, N. Added, G.F. Lima, M.S. Hussein, J. Kolata, and A. Arazi, *Eur. Phys. J. A* 25, 733 (2005).
 - [18] A. Lépine-Szily, R. Lichtenthäler, and V. Guimarães, *Eur. Phys. J. A* 50, 128 (2014).
 - [19] M.P. Kuchera, O.B. Tarasov, D. Bazin, B. Sherril, K. V. Tarasova, *Nucl. Instr. Meth. Phys. Res. B* 376, 168 (2016).
 - [20] <https://github.com/jczamorac/RIBRAS-1>
 - [21] S. Agostinelli and others, *Nucl. Instrum. Meth. Phys. Res. Sec. A*, Volume 506, Issue 3, p. no. 250-303 (2003).
 - [22] J.C. Overley and Ward Whaling, *Phys. Rev.* 128, 315 (1962).
 - [23] M. Freer, N.L. Achouri, C. Angulo, N.I. Ashwood, D.W. Bardayan, S. Brown, W.N. Catford, K.A. Chipps, N. Curtis, P. Demaret, C. Harlin, B. Laurent, J.D. Malcolm, M. Milin, T. Munoz Britton, N.A. Orr, S.D. Pain, D. Price, R. Raabe, N. Soic, J.S. Thomas, C. Wheldon, G. Wilson, and V.A. Ziman, *Phys. Rev. C* 85, 014304 (2012).
 - [24] E.M. Bernstein, *Nucl. Phys.* 59, 525 (1964).
 - [25] A. Kafkarkou, M. W. Ahmed, D. P. Kendellen, I. Mazumdar, J. M. Mueller, L. S. Myers, M. H. Sikora, H. R. Weller, and W. R. Zimmerman, *Phys. Rev. C* 89, 014601 (2014).
 - [26] M. Wiescher, R.N. Boyd, S.L. Blatt, L.J. Rybarczyk, J.A. Spizuoco, R.E. Azuma, E.T.H.

- Clifford, J.D. King, J. Görres, C. Rolfs, and A. Vlieks, Phys. Rev. C 28, 1431 (1983).
- [27] R.B. Day and T. Huus, Phys. Rev. 95, 1003 (1954).
- [28] F. Ajzenberg-Selove and T. Lauritsen, Nuclear Phys. 11, 1 (1959).
- [29] <https://www.nndc.bnl.gov/nudat3/>
- [30] H. Yamaguchi, T. Hashimoto, S. Hayakawa, D. N. Binh, D. Kahl, S. Kubono, Y. Wakabayashi, T. Kawabata, and T. Teranishi, Phys. Rev. C 83, 034306 (2011).
- [31] J. Okołowicz, M. Płoszajczak, and W. Nazarewicz, Phys. Rev. Lett. 124, 042502 (2020).